The official journal of
INTERNATIONAL FEDERATION OF PIGMENT CELL SOCIETIES · SOCIETY FOR MELANOMA RESEARCH

PIGMENT CELL & MELANOMA Research

The PI3K pathway induced by αMSH exerts a negative feedback on melanogenesis and contributes to the release of pigment

Sarah Mosca | Giorgia Cardinali | Enrica Flori | Stefania Briganti | Irene Bottillo | Anna M. Mileo | Vittoria Maresca

DOI: 10.1111/pcmr.12910
Volume 34, Issue 1, Pages 72–88

Received: 23 December 2019 | Revised: 15 June 2020 | Accepted: 22 June 2020

DOI: 10.1111/pcmr.12910

ORIGINAL ARTICLE

WILEY

The PI3K pathway induced by αMSH exerts a negative feedback on melanogenesis and contributes to the release of pigment

Sarah Mosca[1*] | Giorgia Cardinali[1*] | Enrica Flori[1] | Stefania Briganti[1] | Irene Bottillo[2] | Anna M. Mileo[3] | Vittoria Maresca[1]

[1]Laboratory of Cutaneous Physiopathology, San Gallicano Dermatological Institute IRCCS, Rome, Italy

[2]Laboratory of Medical Genetics, Department of Molecular Medicine, San Camillo Forlanini Hospital, Sapienza University of Rome, Rome, Italy

[3]Department of Research Advanced Diagnostic and Technological Innovation – Tumor Immunology and Immunotherapy Unit, IRCCS-Regina Elena National Cancer Institute, Rome, Italy

Correspondence
Vittoria Maresca, San Gallicano Dermatological Institute IRCSS, Laboratory of Cutaneous Physiopathology, Via Elio Chianesi 53, 00144 Rome, Italy.
Email: vittoria.maresca@ifo.gov.it

Funding information
Italian Ministry of Health

Abstract

The melanocortin-1 receptor (MC1R) belongs to the family of the G protein-coupled receptor (GPCR). Activated GPCRs can promote the phosphoinositide 3-kinase (PI3K) pathway. Few studies deal with the role of the PI3K pathway activation in response to αMSH. On B16-F10 cell line, we investigated the αMSH-dependent modulation of pAKT/AKT, as a key element of the PI3K pathway after rapid and prolonged stimulation. We demonstrated that αMSH triggers a rapid modulation of AKT which culminates in an increase in its phosphorylation. We highlighted a comparable up-regulation of pAKT after exposure to αMSH on primary cultures of normal human melanocytes (NHMs) expressing a wild-type MC1R. On B16-F10 cells, NHMs, and an ex vivo model of human skin biopsies, we explored the influence of PI3K/AKT signaling triggered by αMSH, focusing on the control of melanogenesis and pigment release. We showed that the αMSH-dependent PI3K/AKT pathway exerts a negative feedback on melanogenesis and promotes the extracellular release of pigment. We strengthened the role of the PI3K/AKT pathway triggered by αMSH in preserving redox equilibrium and genome integrity, highlighting its role in affecting cell survival.

KEYWORDS

AKT, apoptosis, B16-F10, melanin, melanocytes, melanogenesis, pAKT, PI3K, αMSH

1 | INTRODUCTION

The alpha-melanocyte-stimulating hormone (αMSH) binds the melanocortin-1 receptor (MC1R) and induces the synthesis of melanin (Herraiz, Garcìa-Borron, Jiménez-Cervantes, & Olivares, 2017; Swope & Abdel-Malek, 2016). This effect is a consequence of the cAMP/PKA pathway activation and is strictly regulated by the microphthalmia transcription factor (MITF) (Buscà & Ballotti, 2000; Cheli, Ohanna, Ballotti, & Bertolotto, 2010). Furthermore, the activated form of MC1R triggers other pathways, which also exert extra-melanogenic effects (Cao et al., 2013; Herraiz et al., 2017; Maresca, Flori, & Picardo, 2015). αMSH transactivation of the tyrosine kinase receptors can in turn activate the MAPK/ERK pathway (Herraiz et al., 2011). We demonstrated that αMSH was able to activate PLC (Flori et al., 2017; Maresca et al., 2013), which is known to determine the release of Ca^{++} from endoplasmic reticulum (ER) stores. A relevant study delineated a signaling axis in response to αMSH, which couples cAMP-mediated signaling and Ca^{++} fluxes through the ER calcium sensor protein STIM1 (stromal interaction molecule 1) (Motiani et al., 2018). MC1R is classified as a GPCR (Herraiz et al., 2017; Wolf Horrell, Boulanger,

*Sarah Mosca and Giorgia Cardinali contributed equally to this work.

& D'Orazio, 2016). GPCRs can activate phosphatidylinositol-3-kinase (PI3K) (Burke & Williams, 2015). PI3K phosphorylates phosphatidylinositol-(3,4)-biphosphate (PIP_2) to phosphatidylinositol-(3,4,5)-triphosphate (PIP_3), which can recruit AKT to the cell membrane. When activated by phosphorylation, AKT triggers downstream events which further promote cell survival and proliferation (Carpenter & Cantley, 1996; Cleary & Shapiro, 2010; Franke, Kaplan, & Cantley, 1997; Vanhaesebroeck & Alessi, 2000; Vanhaesebroeck, Whitehead, & Piñero, 2016; Yu & Cui, 2016).

Few studies have evaluated the ability of the activated MC1R to modulate the PI3K pathway, and the data present in the literature, although relevant, are still sporadic (Cao et al., 2013; Castejón-Griñán, Herraiz, Olivares, Jiménez-Cervantes, & Garcìa-Borron, 2018; Cheng et al., 2013; Kadekaro et al., 2005). An important study in this field analyzed the role of αMSH/MC1R interaction in influencing PI3K/PTEN/AKT signaling. In this paper, the authors describe PTEN and its crucial role in protecting against UV-induced melanomagenesis (Cao et al., 2013). A study conducted on NHMs expressing a wild-type MC1R showed that, when the PI3K pathway is inhibited, αMSH reduces its ability to preserve genomic integrity and it becomes ineffective in protecting against apoptosis (Kadekaro et al., 2005). Conversely, a recent paper showed that, during the first phases of MC1R stimulation, NDP-αMSH (a stable αMSH analog) induces AKT phosphorylation in cells carrying MC1R polymorphic variants and this effect is not present in cells expressing a wild-type MC1R (Castejón-Griñán et al., 2018). The PI3K pathway is well known for its ability to promote cell survival as well as tumor progression and aggressiveness (Carpenter & Cantley, 1996; Cleary & Shapiro, 2010; Franke et al., 1997; Vanhaesebroeck & Alessi, 2000; Vanhaesebroeck et al., 2016; Yu & Cui, 2016). The increase in cell survival is detrimental in melanoma because it makes it resistant to medical therapies, but it is crucial for differentiated melanocytes that must resist the insult of ultraviolet radiation.

All these aspects have prompted us to analyze the role of pAKT (as a key element of the PI3K pathway) on B16-F10 cells (murine melanoma) and NHMs. In the aforementioned cell cultures, αMSH exposure triggered a rapid modulation of pAKT levels which culminates in an evident increase; αMSH-dependent PI3K/AKT signaling has been shown to play a key role in the control of both melanogenesis and extracellular release of pigment. The latter aspect was also verified in ex vivo models of human skin explants. Finally, in agreement with previous literature data, we showed that an alteration of this axis can lead to an imbalance in redox equilibrium and, consequently, interference with genomic integrity. These aspects become relevant in the control of cell survival.

Significance

By working on B16-F10 cells, NHMs and an *ex-vivo* model of human skin biopsies, we show that the phosphoinositide 3-kinase (PI3K) pathway induced by the α-Melanocyte stimulating hormone (αMSH) exerts a negative feedback on melanogenesis and contributes to the extracellular release of melanin. Moreover, in agreement with previous literature data, we show that an alteration of this axis can lead to an imbalance in the redox equilibrium and consequently, interference with genomic integrity. The study of these aspects is crucial for improving knowledge on the molecular mechanisms related to cell survival.

2 | MATERIALS AND METHODS

3 | RESULTS

3.1 | The αMSH modulates pAKT levels and its recruitment on the plasma membrane through the PI3K pathway in B16-F10 cells

We performed a time-course analysis of pAKT levels in B16-F10 cells after treatment with 10^{-7} M αMSH for up to 30 min (Figure 1a,b). After 10 min, we observed a significant decrease in protein phosphorylation levels, whereas after 15 and 30 min, the expression of the phosphorylated protein returned to the control values. We then investigated the modulation of pAKT induced by αMSH at later time points (6, 24, and 48 hr) (Figure 1c,d). A significant increase in protein phosphorylation was already observed at 6 hr, reaching a maximum after 24 hr of treatment. Similar results were also obtained by exposing the cells to the αMSH dose of 10^{-8} M for 24 hr (Figure S1). After 48 hr of exposure to the hormone, pAKT levels were similar to those observed in untreated control cells. Moreover, we demonstrated that exposure to the hormone for 24 hr was able to induce the upregulation of both basal and phosphorylated forms of mTOR and S6 as downstream markers of the PI3K pathway (Figure S2). In order to understand whether the effect of αMSH on pAKT induction was dependent on the PI3K pathway, we investigated the modulation of pAKT levels in B16-F10 treated with αMSH for 24 hr in the presence or absence of 10 μM LY294002, a PI3K inhibitor (Ohashi & Woodgett, 2005; Yu & Cui, 2016). We confirmed that αMSH was able to promote an increase in pAKT levels after 24 hr and that this effect was hindered by the presence of the LY294002 (Figure 1e,f). We obtained similar results by employing Wortmannin, another PI3K inhibitor (Oka et al., 2000) (Figure 1g,h). Finally, we investigated the localization of pAKT by immunofluorescence analysis (Figure 2a,b). We demonstrated that αMSH exposure for 24 hr induced an increase in the expression of pAKT associated with an evident localization on the plasma membrane. These effects decreased significantly when the cells were exposed to αMSH in combination with LY294002.

3.2 | The αMSH-dependent PI3K/AKT pathway exerts a great influence on dendricity and pigmentation in B16-F10 cells

We stimulated B16-F10 cells with αMSH, LY294002, or αMSH plus LY294002 for 24, 48, and 72 hr, and morphological changes were checked over time (Figure 3). As expected, B16-F10 cells stimulated with αMSH showed a gradual increase in pigmentation. In agreement with previous studies (Buscà, Bertolotto, Ortonne, & Ballotti, 1996;

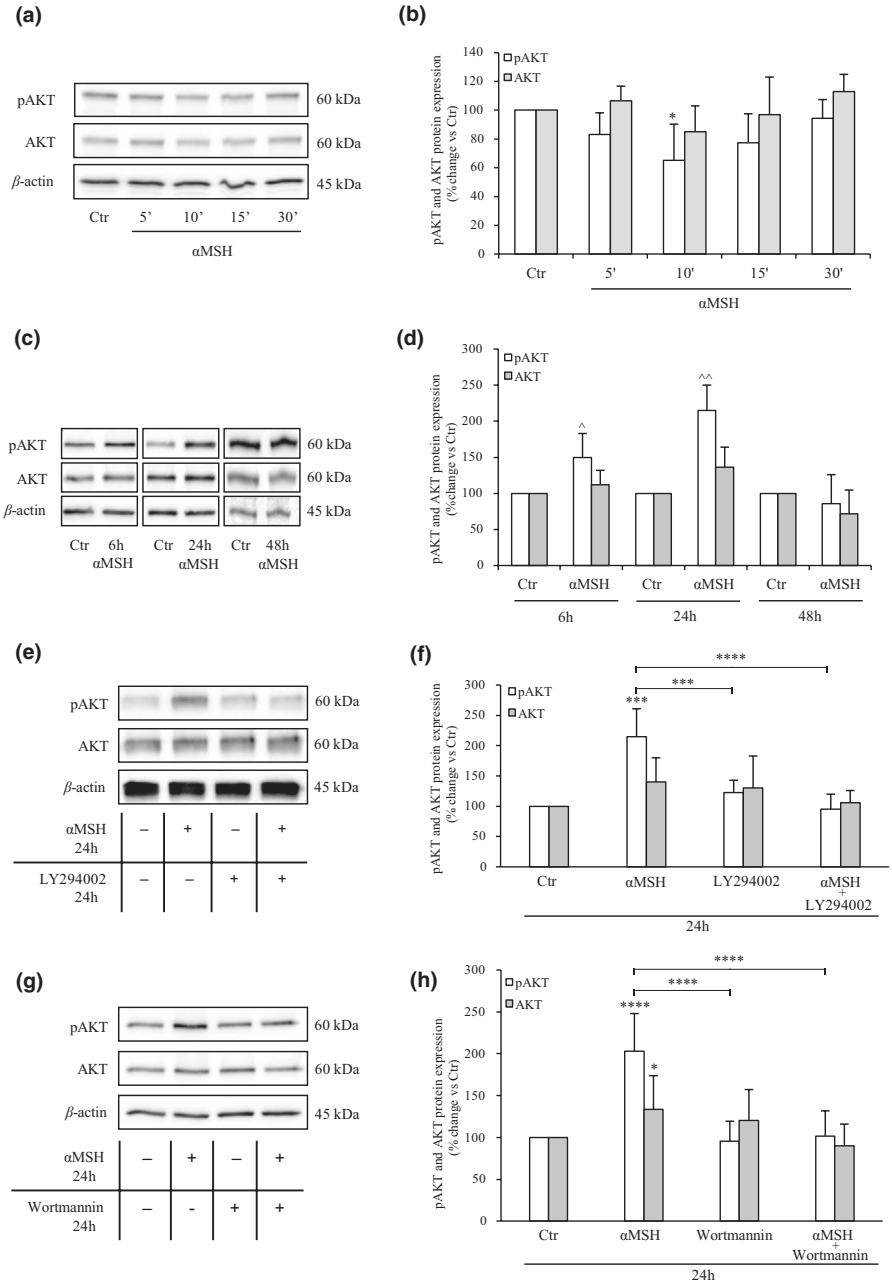

FIGURE 1 αMSH modulates pAKT levels through the PI3K pathway in B16-F10 cells. (a) Western blot analysis of pAKT and AKT protein expression on cell lysate of B16-F10 treated with 10^{-7} M αMSH for 5, 10, 15, and 30 min. Representative blots are shown. (b) Densitometric scanning of band intensities was performed to quantify the change in protein expression. One-way ANOVA with post hoc Tukey's tests: $^{*}p < .05$ (versus untreated control cells). (c) Western blot analysis of pAKT and AKT protein expression on cell lysate of B16-F10 treated with 10^{-7} M αMSH for 6, 24, and 48 hr. Representative blots are shown. (d) Densitometric scanning of band intensities was performed to quantify the change in protein expression. Student's *t* test: $^{\wedge}p < .05$ and $^{\wedge\wedge}p < .01$ (versus untreated control cells). (e) Western blot analysis of pAKT and AKT protein expression on cell lysate of B16-F10 treated with 10^{-7} M αMSH for 24 hr in the presence or absence of 10 μM LY294002. Representative blots are shown. (f) Densitometric scanning of band intensities was performed to quantify the change in protein expression. One-way ANOVA with post hoc Tukey's tests: $^{***}p < .001$ and $^{****}p < .0001$. (g) Western blot analysis of pAKT and AKT protein expression on cell lysate of B16-F10 treated with 10^{-7} M αMSH for 24 hr in the presence or absence of 10 μM Wortmannin. Representative blots are shown. (H) Densitometric scanning of band intensities was performed to quantify the change in protein expression. One-way ANOVA with post hoc Tukey's tests: $^{*}p < 0.$ and $^{****}p < .0001$

Englaro et al., 1998), a similar effect was also observed in response to LY294002 exposure. Furthermore, the cells exposed to LY294002 for 72 hr showed an elongated and spinous phenotype, characterized by the presence of dendrites visibly loaded with melanin. Combined treatment with αMSH plus LY294002 induced a more pronounced effect on both pigmentation and dendricity, in comparison with that

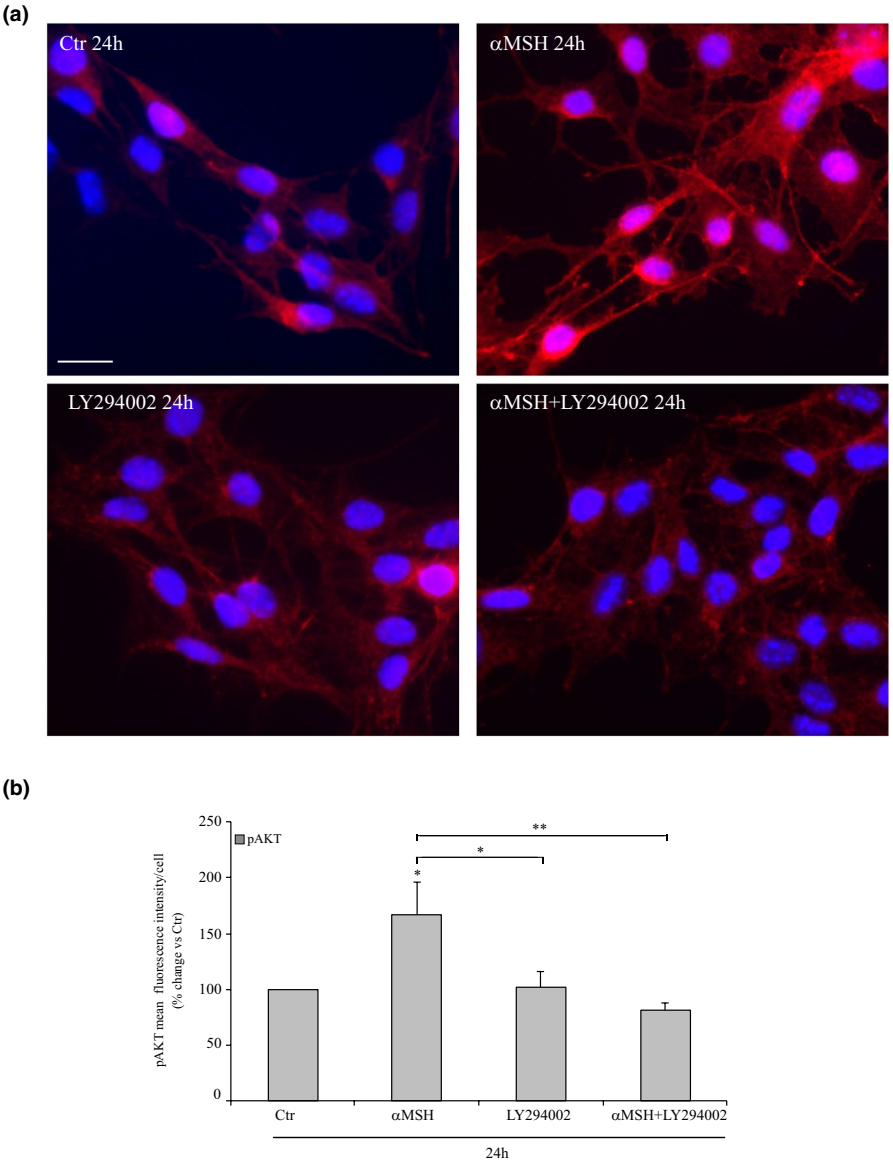

FIGURE 2 αMSH modulates pAKT recruitment on the plasma membrane through the PI3K pathway in B16-F10 cells. (a) Immunofluorescence analysis of pAKT (red) localization on B16-F10 cells treated with 10^{-7} M αMSH for 24 hr in the presence or absence of 10 μM LY294002. Nuclei are counterstained with DAPI. Scale bar: 20 μm. (b) Quantitative analysis of pAKT fluorescence intensity. Results are expressed as fold increase in mean fluorescence intensity/cell with respect to the value obtained in untreated control cells (set as 100 by definition) and are reported as mean value (%) ± *SD*. One-way ANOVA with post hoc Tukey's tests: $^{*}p < .05$ and $^{**}p < .01$

exerted by the single agents. This potentiated effect reached a peak at 72 hr. We performed experiments of AKT gene silencing (Figure 4) in order to rule out the possibility that the accumulation of melanin, after combined treatment, was ascribable to an LY294002 side effect (Brunn et al., 1996). We evaluated the AKT protein expression in B16-F10 transiently transfected with siRNA for AKT1 (siAKT) or control (siCtr) (Figure 4a,b). We stimulated AKT-silenced B16-F10 cells for 24 hr with αMSH, LY294002, or αMSH plus LY294002, and we analysed the changes on cell morphology over time (Figure 4c,d). In the siCtr cells treated with αMSH plus LY294002, we confirmed the presence of pigment clusters on the tips of dendrites. As expected, we observed the same pigment clusters in cells that were transfected with siAKT and then exposed to αMSH. Therefore, we highlighted the role of the αMSH-dependent PI3K-AKT pathway as a negative regulator of differentiation in B16-F10 cells through both the pharmacological inhibition of PI3K and the silencing of the AKT gene.

3.3 | The αMSH-dependent PI3K/AKT pathway downregulates the expression of MITF in B16-F10 cells

Since the agents we employed caused evident effects on cell pigmentation (particularly, the combined treatment), we focused our study on MITF expression (Figure 5). We confirmed that the B16-F10 cell line responded to αMSH via MITF upregulation (Cheli et al., 2010) (Figure 5a,b). More in detail, we performed a time-course analysis of MITF expression until 48 hr of exposure to αMSH and we observed a significant upregulation of the protein at 2 hr and 3 hr of treatment. We evaluated the effect of the treatment with αMSH plus LY294002 at 3 hr, and we observed that the combined treatment led to an even more evident upregulation of MITF (Figure 5c,d). These results indicated that the αMSH-dependent PI3K pathway promoted a negative effect on MITF expression.

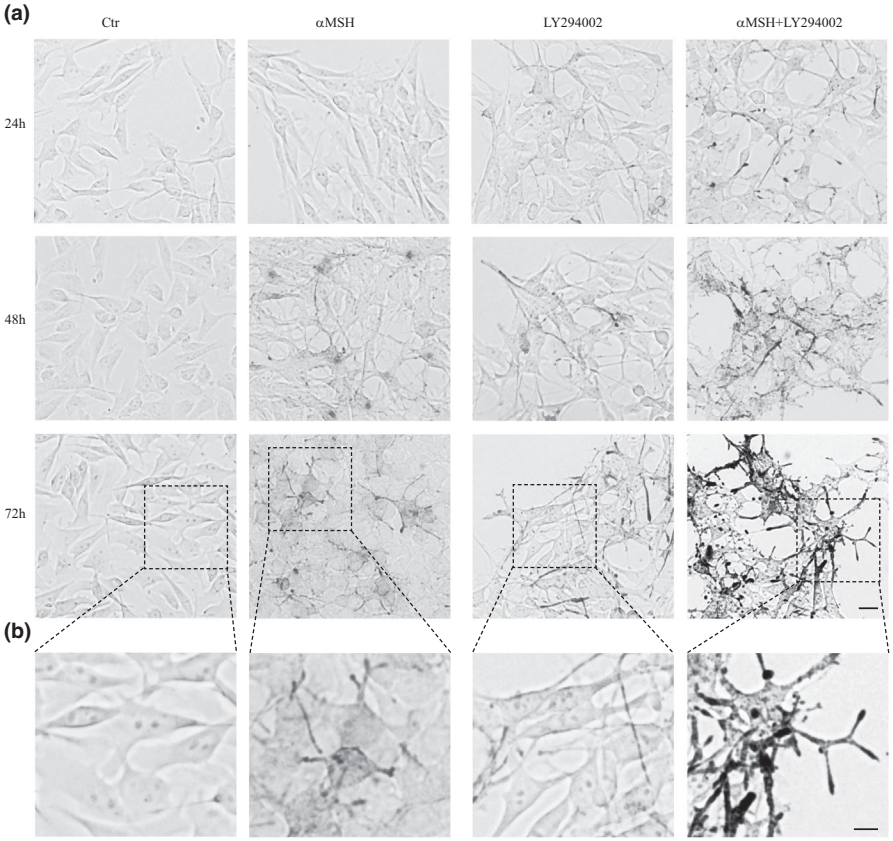

FIGURE 3 The αMSH-dependent PI3K/AKT pathway exerts a great influence on the dendricity and pigmentation of B16-F10 cells. (a) Phase-contrast analysis of B16-F10 cells treated with 10^{-7} M αMSH for 24, 48, and 72 hr in the presence or absence of 10 μM LY294002. Scale bar: 50 μm. (b) Images showing the boxed areas in panel a (72 hr of treatment) at higher magnification. Scale bar: 25 μm

3.4 | The αMSH-dependent PI3K/AKT pathway downregulates the expression and activity of tyrosinase in B16-F10 cells

We then focused on tyrosinase expression and activity which represents the main target of the MITF transcription factor. We evaluated tyrosinase mRNA expression in response to αMSH, LY294002, or αMSH plus LY294002 treatment for 6 and 24 hr: Both αMSH and LY294002 promoted a significant increase in mRNA for tyrosinase at 24h and the combined treatment potentiated this effect at both time points evaluated (Figure 6a). We also analyzed the tyrosinase expression profile after 6, 24, and 48 hr of exposure to αMSH (Figure 6b,c). We observed a significant increase in the enzyme at every time points evaluated, with a maximum expression after 48 hr. At 24 hr, the effect of the αMSH plus LY294002 combined treatment on tyrosinase expression was even more relevant (Figure 6d,e). Finally, we analyzed the effects of the different treatments at 24, 48, and 72 hr on tyrosinase activity (Figure 6f). αMSH promoted a significant increase in tyrosinase activity already at 24 hr of treatment; a greater enzymatic activity was promoted in response to LY294002, and this effect was even more evident in response to αMSH plus LY294002. These effects were enhanced after 48 hr and reached a maximum level after 72 hr, suggesting that the αMSH-dependent PI3K pathway exerted a negative effect on tyrosinase activity.

3.5 | The αMSH-dependent PI3K/AKT pathway downregulates the synthesis of melanin and facilitates the release of pigment outside B16-F10 cells

We evaluated the total intracellular amount of melanin after stimulation with αMSH, LY294002, or αMSH plus LY294002, for 24, 48, and 72 hr (Figure 7a). After 24 hr of treatment, αMSH already promoted a significant increase in the amount of intracellular melanin; a greater amount of melanin was induced in response to LY294002, and this effect was even more evident in response to the αMSH plus LY294002 treatment. Following the treatment with LY294002 and with αMSH plus LY294002, these effects were enhanced after 48 hr and reached a maximum level after 72 hr. As shown in Figure 7b, the culture medium of the samples, after exposure to different treatments for 72 hr, appeared in different colors. In cells exposed to αMSH, the culture medium appeared darker than that observed in untreated control cells, in agreement with the increased synthesis of melanin induced by the hormone. Surprisingly, in cells exposed to LY294002 or combined treatment, the amount of pigment released into the culture medium did not increase in parallel to the intracellular increase in melanin.

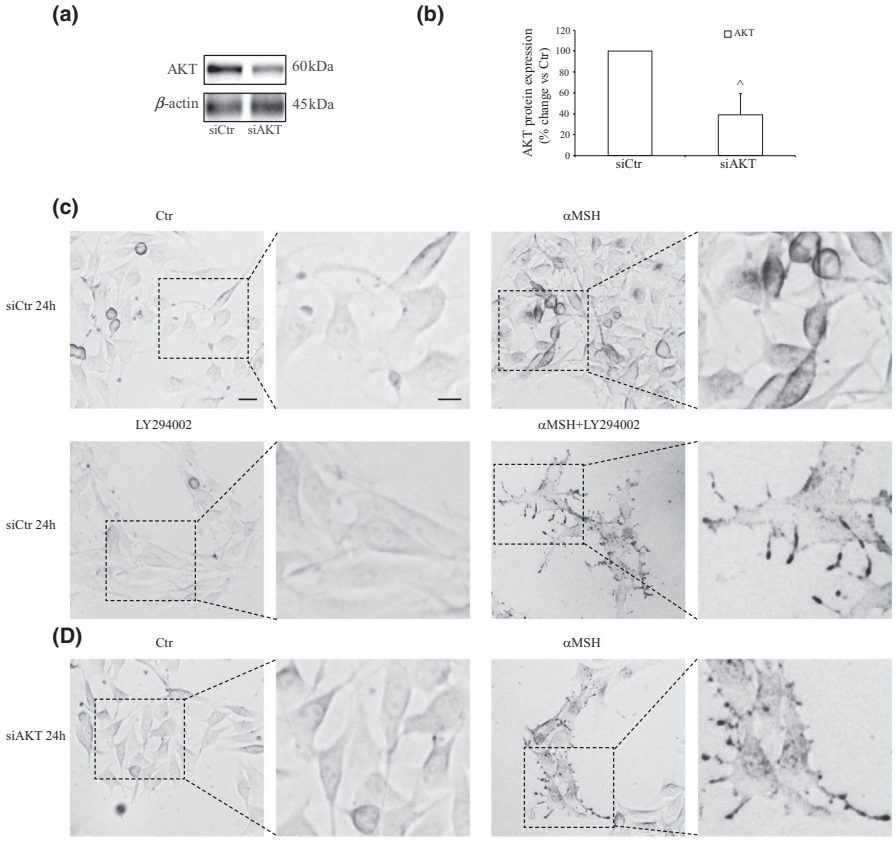

FIGURE 4 The αMSH-dependent PI3K/AKT pathway strictly acts on cell dendricity and pigmentation. (a) B16-F10 cells were transfected with specific siRNA for the AKT gene (siAKT) or non-specific siRNA (siCtr). AKT protein expression level was evaluated by Western blot. (b) Densitometric scanning of band intensities was performed to quantify the change in AKT protein expression after 24 hr. Student's *t* test: $^p < .05$ (versus siCtr cells). (c) Phase-contrast analysis of B16-F10 cells transfected with siCtr and then treated with 10^{-7} M αMSH for 24 hr in the presence or absence of 10 μM LY294002. (d) Phase-contrast analysis of B16-F10 cells transfected with siAKT and then treated with 10^{-7} M αMSH for 24 hr. The higher magnifications of boxed areas are shown in panels (c) and (d) to highlight the differences in melanin distribution. Scale bars: 50 μm and 25 μm for low magnification and high magnification, respectively

3.6 | The modulation of PAKT triggered by αMSH is conserved also in NHMs

Some evaluations performed on B16-F10 cells were also extended to NHMs, which represent a physiological cellular context. On NHMs expressing the wild-type MC1R, which respond to αMSH in terms of tyrosinase over-expression (Figure 8a,b), we performed a time-course analysis of pAKT levels in response to the αMSH stimulus (Figure 8c,d). On these cells, αMSH promoted a significant decrease in protein phosphorylation at 15 and 30 min of treatment (Figure 8c-e). We observed an inverse trend at longer exposure times to αMSH: In fact, pAKT resulted significantly upregulated after 24 and 48 hr of hormonal treatment (Figure 8d-f).

3.7 | The αMSH-dependent PI3K/AKT pathway exerts a great influence on dendricity and pigmentation in NHMs

We stimulated NHMs with αMSH, LY294002, or αMSH plus LY294002 for 24, 48, and 72 hr, and we observed changes in cell morphology over time (Figure 9a,b). NHMs exposed to αMSH showed a gradual change in cell shape. Treatment with LY294002 did not change cell morphology, whereas co-treatment with αMSH plus LY294002 caused an increase in dendricity, which is associated with an evident clusterization of melanin. These effects reached a peak at 72 hr of treatment. Based on these observations, we evaluated the total intracellular amount of melanin after stimulation with αMSH, LY294002, or αMSH plus LY294002 for 24, 48, and 72 hr (Figure 9c). A significant increase in intracellular melanin was observed after exposure to αMSH for 24 hr. A significant increase in intracellular melanin was seen after 72 hr in response to LY294002. The longer the exposure time to αMSH plus LY294002, the more melanin levels increased. Moreover, after combined treatment, and starting from 48 hr, the intracellular melanin amount resulted significantly increased in comparison with both the untreated control cells and the cells treated with agents employed alone.

3.8 | The αMSH-dependent PI3K/AKT pathway is involved in the release of melanosomes in ex vivo human skin models

The most intriguing aspect of this study is the αMSH-dependent PI3K pathway's involvement in promoting the extracellular release of melanosomes. On this basis, we proceeded to evaluate this aspect on ex vivo human skin explants. Skin explants were exposed to αMSH, LY294002, or αMSH plus LY294002 for five days. Histological analysis by H&E staining did not reveal changes in epidermal morphology following treatments (Figure 10a). We performed immunohistochemical analysis using an antibody against Melan A as a melanosomal antigen to identify melanosome content and distribution (Figure 10b,c). In the αMSH-treated sample, we observed an increase in melanosome distribution on keratinocytes surrounding

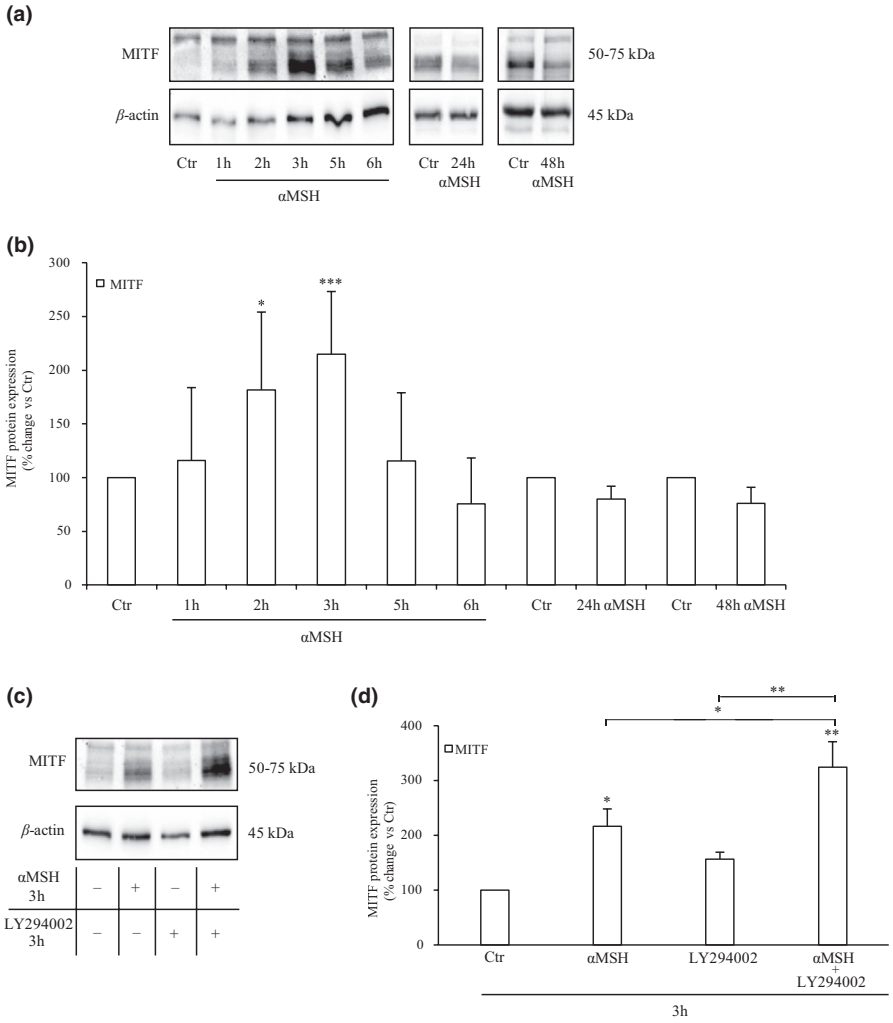

FIGURE 5 The αMSH-dependent PI3K/pAKT downregulates MITF expression in B16-F10 cells. (a) Western blot analysis of MITF protein expression on cell lysate of B16-F10 treated with 10^{-7} M αMSH for 1, 2, 3, 5, 6, 24, and 48 hr. Representative blots are shown. (b) Densitometric scanning of band intensities was performed to quantify the change in protein expression. One-way ANOVA with post hoc Tukey's tests: $^{*}p < .05$ and $^{***}p < .001$ (versus untreated control cells). (c) Western blot analysis of MITF protein expression on cell lysate of B16-F10 treated with 10^{-7} M αMSH for 3 hr, in the presence or absence of 10 μM LY294002. Representative blot is shown. (d) Densitometric scanning of band intensities was performed to quantify the change in protein expression. One-way ANOVA with post hoc Tukey's tests: $^{*}p < .05$ and $^{**}p < .01$

positive melanocytes. In response to LY294002 and even more so in response to αMSH plus LY294002, we observed a significant increase in the punctate staining pattern inside melanocytes, which suggests a phenomenon of melanosome retention (Figure 10c), confirming the results obtained on cell cultures.

3.9 | The αMSH-dependent PI3K/PAKT pathway contributes to protection against oxidative stress and apoptosis

The PI3K/pAKT pathway is involved in regulating antioxidant responses (De Nicola et al., 2011; Koundouros & Poulogiannis, 2018; Sporn & Liby, 2012); thus, we decided to evaluate the redox state following the different treatments. We analyzed ROS production in NHMs after 24, 48, and 72 hr of stimulation with αMSH, LY294002, or αMSH plus LY294002 (Figure 11a). αMSH exposure did not produce a significant increase in ROS after 24 hr. Indeed, it determined a gradual protection against oxidative stress at 72h. Regardless of the period of time analyzed, LY294002 did not produce any significant variation in the amount of ROS. In comparison with untreated cells, combined treatment with αMSH plus LY294002 generated a significant ROS increase exclusively after 24 hr. At later times, combined treatment gradually decreased the ROS amount. These results demonstrated that, in NHMs, the αMSH-mediated PI3K/AKT pathway played a role in protecting against oxidative damage in association with other possible protective mechanisms.

In parallel, we also evaluated ROS production on B16-F10 (Figure 11b). A significant increase in ROS was observed in response to treatment with LY294002 at all times analyzed. At all evaluation time points, the combined treatment with αMSH plus LY294002 determined a synergistic effect on ROS production, which peaked at 72 hr (Figure 11b).

Based on these results, we wondered whether the generated ROS could have an impact on DNA integrity. To this end, we investigated the expression of gamma-H2AX (γH2AX), as a marker of DNA double-strand breaks (Yuan, Adamski, & Chen, 2010), on cells exposed to the above-described stimuli for 24, 48, and 72 hr (Figure 12a,b). At all analyzed time points, αMSH did not induce significant changes in the γH2AX protein expression. As expected, LY294002, which is able to induce apoptosis (Kadekaro et al., 2005), caused a significant over-expression of γH2AX but only after 72 hr of treatment. Co-treatment with αMSH plus LY294002 significantly

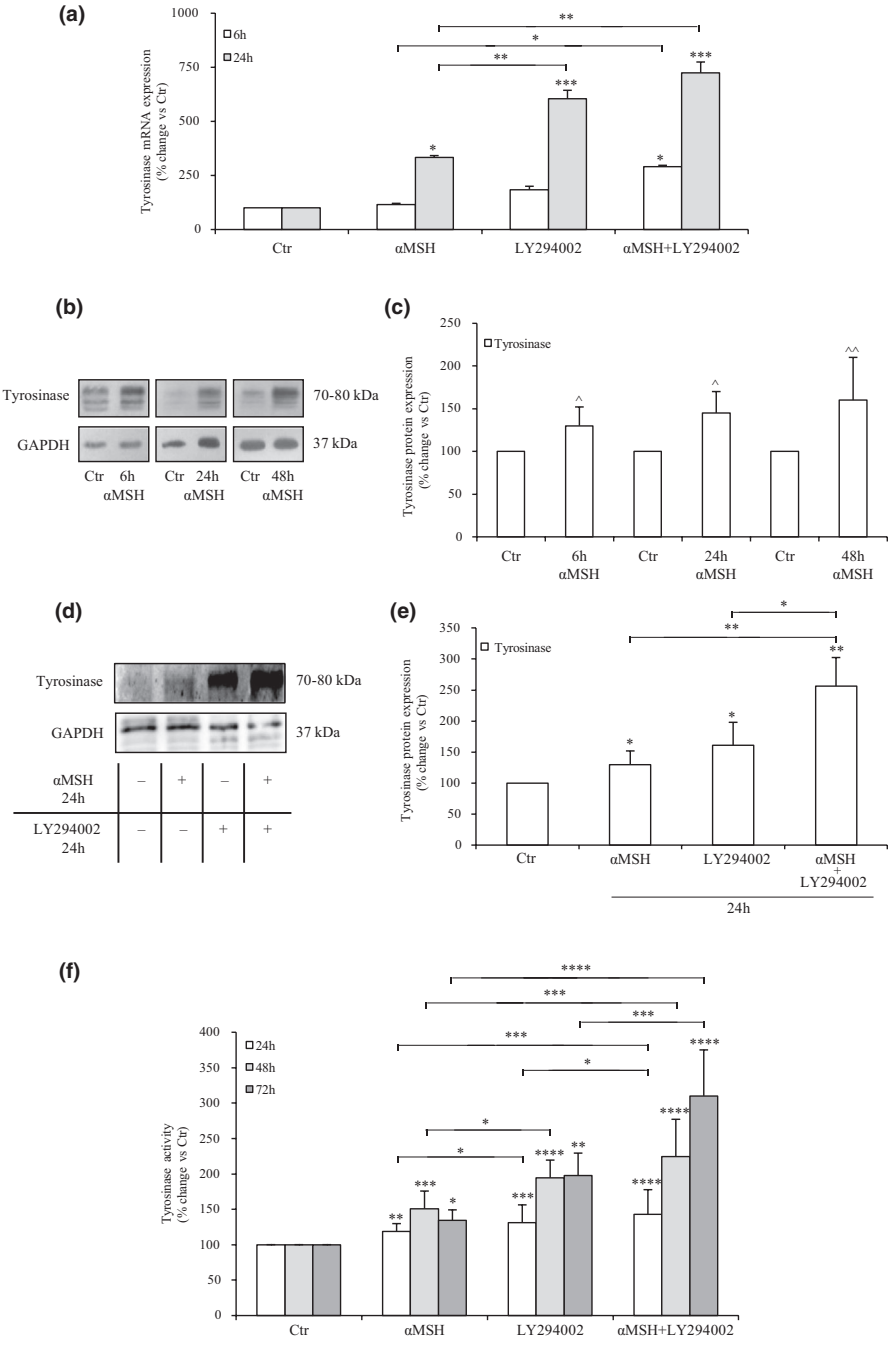

FIGURE 6 The αMSH-dependent PI3K/pAKT pathway downregulates tyrosinase expression in B16-F10 cells. (a) Analysis of tyrosinase mRNA expression on B16-F10 treated with 10^{-7} M αMSH in the presence or absence of 10 μM LY294002 for 6 and 24 hr. One-way ANOVA with post hoc Tukey's tests: $^{*}p < .05$, $^{**}p < .01$, and $^{***}p < .001$. (b) Western blot analysis of tyrosinase protein expression on cell lysate of B16-F10 treated with 10^{-7} M αMSH for 6, 24, and 48 hr. Representative blot is shown. (c) Densitometric scanning of band intensities was performed to quantify the change in protein expression. Student's *t* test: $^{\wedge}p < .05$ and $^{\wedge\wedge}p < .01$ (versus untreated control cells). (d) Western blot analysis of tyrosinase protein expression on cell lysate of B16-F10-treated with 10^{-7} M αMSH for 24 hr in the presence or absence of 10 μM LY294002. Representative blot is shown. (e) Densitometric scanning of band intensities was performed to quantify the change in protein expression. One-way ANOVA with post hoc Tukey's tests: $^{*}p < .05$ and $^{**}p < .01$. (f) Analysis of tyrosinase activity on B16-F10 treated with 10^{-7} M αMSH in the presence or absence of 10 μM LY294002 for 24, 48, and 72 hr. One-way ANOVA with post hoc Tukey's tests: $^{*}p < .05$, $^{**}p < .01$, $^{***}p < .001$, and $^{****}p < .0001$

increased the expression levels of γH2AX at 48 hr. This effect was even more pronounced at 72 hr.

Since LY294002 is able to induce apoptosis, we wondered whether combined treatment with αMSH plus LY294002 (which was able to generate a big amount of ROS) was also able to promote a similar effect of cell death. To this end, we analyzed the expression of procaspase-3 on the B16-F10 cell line in response to different treatments for 72 hr (Figure 12c,d). As expected, we observed a decrease in procaspase-3 expression following LY294002 exposure (see also Figure S3), and this effect was even more pronounced after combined treatment with αMSH plus LY294002.

4 | DISCUSSION

Only few studies in literature deal with the analysis of the PI3K pathway and its effects in cells which synthesize melanin (Cao et al., 2013; Castejón-Griñán, Herraiz, Olivares, Jiménez-Cervantes, & Garcìa-Borron, 2018; Cheng et al., 2013; Kadekaro et al., 2005). This fact induced us to analyze the behavior of AKT and its activation as a key element of the PI3K pathway, in response to αMSH exposure, in B16-F10 cells and NHMs. A latency phase was observed in these cell lines before the AKT was phosphorylated. In consonance with a previous paper (Khaled et al., 2003), we observed a mild but significant downregulation of pAKT in the early phases of αMSH stimulation. In B16-F10 cells, the AKT protein started to

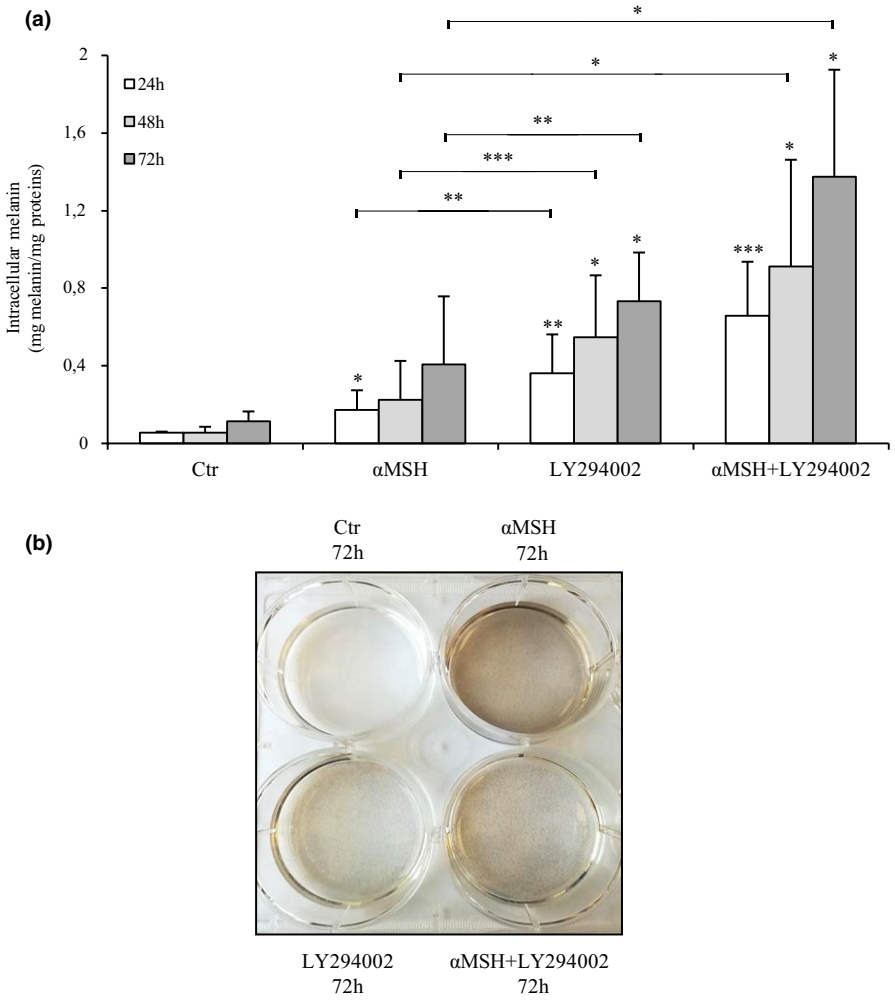

FIGURE 7 The αMSH-dependent PI3K/AKT pathway downregulates the synthesis of melanin and facilitates its extracellular release. (a) Intracellular melanin evaluation in B16-F10 cells treated with 10^{-7} M αMSH in the presence or absence of 10 μM LY294002 for 24, 48, and 72 hr. The melanin content was normalized on total protein content, and results were expressed as mg melanin/mg proteins. One-way ANOVA with post hoc Tukey's tests: $^{*}p < .05$, $^{**}p < .01$, and $^{***}p < .001$. (b) Medium color changes due to melanin extracellular release after treatment with 10^{-7} M αMSH in the presence or absence of 10 μM LY294002 at 72 hr

be upregulated after 6 hr of exposure to the hormone, and both B16-F10 and NHMs showed a significant increase in pAKT levels after 24 hr. As a member of the GPCR family, the MC1R undergoes desensitization and internalization after stimulation with αMSH. The desensitizing effect on the receptor occurs at rapid exposure times to the hormone. This effect is mediated by a mechanism that is PKA-independent and G protein-coupled receptor kinase (GRK)-dependent (Sánchez-Laorden, Jiménez-Cervantes, & García-Borrón, 2007; Swope et al., 2012; Wolf Horrel *et al*., 2016). The effect of desensitization is dependent upon GRK2 and GRK6, and internalization only requires the GRK6-mediated phosphorylation at specific amino acid residues localized in the C-terminal region of MC1R (Sánchez-Laorden et al., 2007). A recent study, carried out on human melanoma cell lines, has clearly described an antagonism between cAMP generation and AKT activation (Castejón-Griñán et al., 2018). The high levels of cAMP, which are generated soon after the activation of the MC1R, prevent the activation of AKT by phosphorylation. Subsequently, the MC1R decouples from the G protein, and only in this phase, AKT phosphorylation can occur. Furthermore, it is worth noting that pAKT levels in untreated cells were higher at 48 hr than 6 hr, suggesting that AKT might be activated slowly even in the absence of stimulation with αMSH. We hypothesize that this effect could be a consequence of the sub-confluence reached by the cells, and it could be ascribed to a mechanism of autocrine regulation triggered by bioactive molecule.

In order to understand whether the effect of αMSH on pAKT induction was dependent on the PI3K pathway, we analyzed the modulation of pAKT in B16-F10 exposed to αMSH in the presence or absence of LY294002 or Wortmannin, two PI3K inhibitors. Both inhibitors reversed the upregulation of pAKT promoted by αMSH alone, thus demonstrating the involvement of PI3K in mediating the activation of AKT. Furthermore, we demonstrated that the inhibition of the PI3K pathway was also involved in the translocation of pAKT to the plasma membrane. It is worth noting that, in the absence of αMSH, pAKT levels were not downregulated through treatment with LY294002 or Wortmannin. This result was somewhat surprising. In the past, both LY294002 and Wortmannin have been described as potent pan-PI3K inhibitors, but more recently they were found to have shortcomings (Cleary & Shapiro, 2010). Eight classes of PI3Ks are currently known. These are active in regulating the most varied biological functions and thus in contributing toward increase in cellular well-being and survival (Carpenter & Cantley, 1996; Cleary & Shapiro, 2010; Franke et al., 1997; Vanhaesebroeck & Alessi, 2000; Vanhaesebroeck et al., 2016; Yu & Cui, 2016). These isoforms work in an integrated way and can therefore compensate each other (Costa et al., 2015; Schwartz et al., 2015). On this basis, we think that

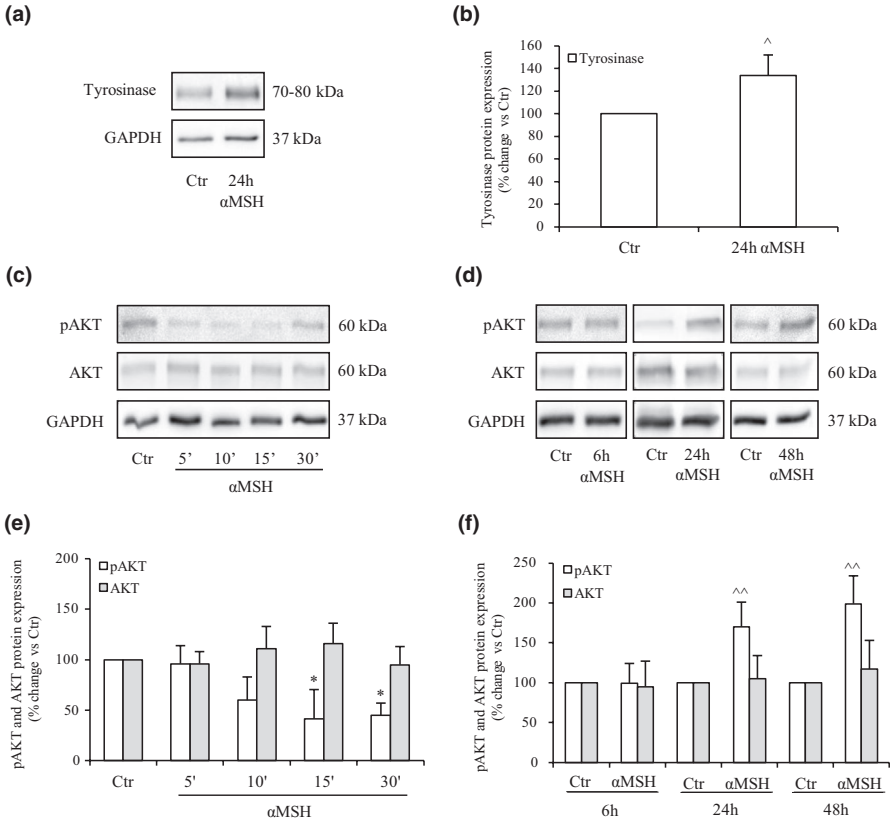

FIGURE 8 Modulation of the pAKT triggered by αMSH is conserved also in NHMs. (a) Western blot analysis of tyrosinase protein expression on cell lysate of NHMs treated with 10^{-7} M αMSH for 24 hr. Representative blot is shown. (b) Densitometric scanning of band intensities was performed to quantify the change in protein expression. Student's *t* test: ^$p < .05$ (versus untreated control cells). (c) Western blot analysis of pAKT and AKT expression on cell lysate of NHMs treated with 10^{-7} M αMSH for 5, 10, 15, and 30 min and (d) 6, 24, and 48 hr. Representative blots are shown. (e,f) Densitometric scanning of band intensities was performed to quantify the change in protein expression. One-way ANOVA with post hoc Tukey's tests: *$p < .05$ (versus untreated control cells). Student's *t* test: ^^$p < .01$ (versus untreated control cells)

24 hr of exposure to LY294002 (or Wortmannin) was long enough to allow cancer cells, such as B16-F10, to implement a compensatory strategy.

Furthermore, we evaluated the effects of αMSH, LY294002 and combined treatment on cell morphology on B16-F10 cells and NHMs. Exposure to αMSH determined a deep morphological change over time, associated with an increase in cell pigmentation. The αMSH plus LY294002 combined treatment potentiated cell differentiation features, with evident pigment clusters inside the elongated dendrites. We employed an AKT gene silencing approach in order to demonstrate a direct relationship between PI3K signaling and pigmentation induced by αMSH. AKT-silenced B16-F10 cells treated with αMSH showed a change in cell morphology very similar to that induced by the αMSH plus LY294002 combined treatment. These results confirmed the involvement of the αMSH-dependent PI3K-AKT pathway in mediating morphological changes.

We investigated the molecular basis of increased melanogenesis on B16-F10 cells, through the analysis of MITF, tyrosinase, and the intracellular melanin content, as the final product of the process. As expected, cells treated with αMSH responded with a positive modulation of all these parameters. Similar results to those reported in previous studies were obtained in the response to LY294002 (Buscà et al., 1996; Englaro et al., 1998). The LY294002-mediated melanogenic response was closely linked to the inhibition of the PI3K pathway. In fact, these effects were previously described in response to the PI3K inhibitor Wortmannin (Oka et al., 2000). However, in our experiments, the pro-melanogenic effect of LY294002 was amplified by co-treatment with αMSH which is able to trigger cAMP/PKA signaling, the canonical pathway of the activated MC1R. Therefore, it is evident that the PI3K pathway, induced by αMSH, exerts a negative feedback on the melanogenesis induced by the cAMP/PKA pathway. In agreement with these results, we observed the presence of melanin clusters in NHM cultures following combined treatment with αMSH plus LY294002. We also demonstrated that intracellular melanin levels were statistically higher in comparison with those detected in the samples only treated with αMSH. These results highlight the role of the αMSH-dependent PI3K pathway in the melanin release process. The retention of melanin, following treatment with αMSH plus LY294002, was also confirmed in human ex vivo skin explants through the immune-histochemical evaluation of the Melan A signal, a melanosomal marker.

Since both the B16-F10 and the NHM cell lines treated with αMSH plus LY294002 were so loaded with melanin and showed profound changes in cell morphology, we wondered whether these aspects were associated with an increase in the radical species. We performed an analysis on the generation of free radical species on NHMs after stimulation with αMSH, alone or in combination with LY294002. The cells' exposure to αMSH resulted in a significant reduction in the ROS amount, and these results concur with previous studies (Castejón-Griñán et al., 2018; Kadekaro et al., 2005; Maresca et al., 2010, 2015). In the same cell lines, the inhibition of the PI3K pathway did not cause an increase in the radical species in any of the observation times. Treatment for 24 hr with αMSH in the presence of LY294002 increased the ROS amount significantly, but, subsequently, the cells were able to buffer it. This result showed that, in

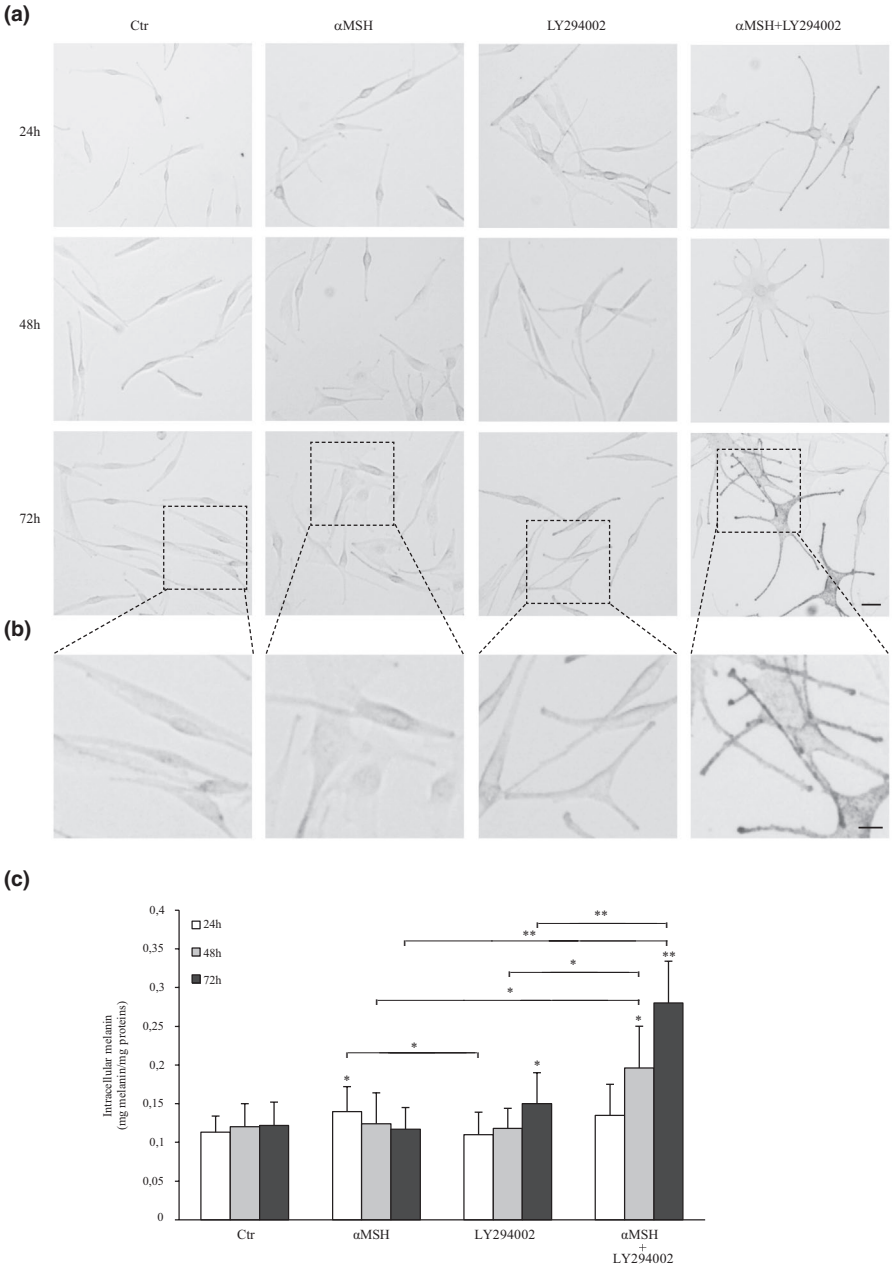

FIGURE 9 The αMSH-dependent PI3K/AKT pathway exerts a great influence on dendricity and pigmentation in NHMs. (a) Phase-contrast analysis of NHMs treated with 10^{-7} M αMSH for 24, 48, and 72 hr in the presence or absence of 10 μM LY294002. The higher magnifications of boxed areas in panel (a) are shown in panel (b) to highlight the differences in melanin distribution. Scale bars: 50 μm and 25 μm for low magnification and high magnification, respectively. (c) Intracellular melanin evaluation in NHMs treated with 10^{-7} M αMSH in the presence or absence of 10 μM LY294002 for 24, 48, and 72 hr. The melanin content was normalized on total protein content, and results were expressed as mg/mg. One-way ANOVA with post hoc Tukey's tests: $^{*}p < .05$ and $^{**}p < .01$

NHMs, the PI3K pathway played a marginal role in the antioxidant protection promoted by αMSH. In fact, this protection is mainly guaranteed by the cAMP/PKA pathway, through the induction of detoxifying enzymes such as the catalase (Maresca et al., 2010, 2015).

In the B16-F10 cell line, treatment with LY294002 alone resulted in a significant increase in the ROS amount, which was directly proportional to the exposure time, and this result was different from that observed in NHMs. The PI3K pathway plays a crucial role in triggering and supporting metabolic rewiring associated with cancer (Carpenter & Cantley, 1996; Cleary & Shapiro, 2010; Franke et al., 1997; Vanhaesebroeck & Alessi, 2000; Vanhaesebroeck et al., 2016; Yu & Cui, 2016). Cancer cells implement their metabolism to ensure they have an adequate energy supply to support tumor proliferation and progression. The generation of ROS is a consequence of this extensive metabolic rewiring. Since excessive ROS would damage proteins, DNA, and cell membranes, a concomitant increase in antioxidant abilities is necessary to restore the redox homeostasis. The Keap-1-Nrf2 pathway and the modulation of glutathione metabolism are protective strategies involved, and they are both regulated by the PI3K/AKT signaling (De Nicola et al., 2011; Koundouros & Poulogiannis, 2018; Sporn & Liby, 2012). Therefore, the PI3K pathway is able to support all the above-mentioned needs due to its well-known ability to promote survival. The amount of ROS resulted in increasingly enhanced after combined treatment with αMSH plus LY294002. It is possible to speculate that, in the B16-F10 cell line, αMSH added a further metabolic burden and a generation of free radical species as side products, to the already intense basal metabolism of the transformed condition.

In B16-F10 cells, we also investigated the possible connection between ROS generation, the damage to DNA, and ultimately,

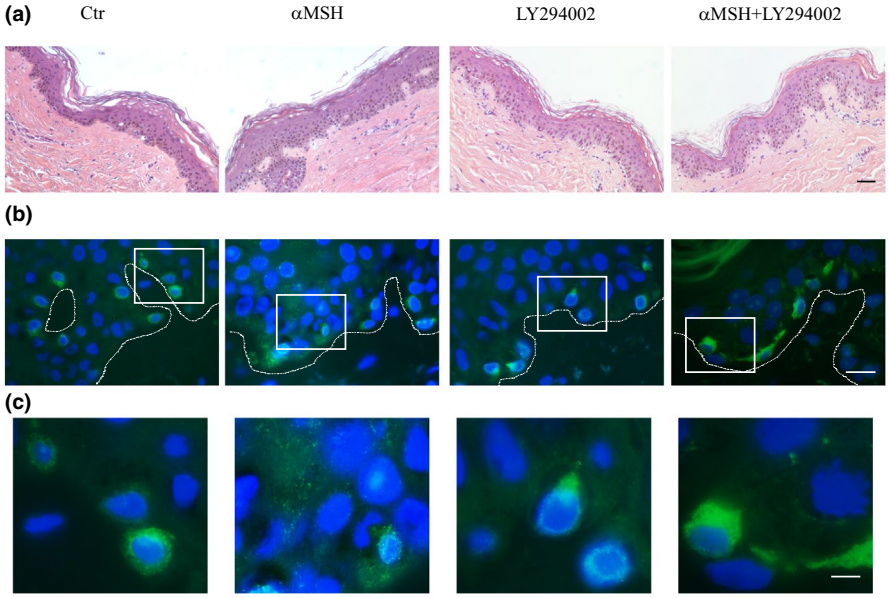

FIGURE 10 The αMSH-dependent PI3K/AKT pathway is involved in the release of melanosomes in an ex vivo human skin model. The ex vivo skin explants were maintained in medium culture at air–liquid interface and were treated with 10^{-7} M αMSH, 10 μM LY294002, and αMSH plus LY294002 for five days. (a) Morphological analysis by hematoxylin and eosin staining on paraffin sections. (b) Immunohistochemical staining for Melan A expression. (c) The higher magnifications of the boxed areas in panel (b) show the differences on punctate staining patterns which reflect a different distribution of melanosomes after the treatments. Nuclei are stained with DAPI. Scale bars: (a) 50 μm, (b) 10 μm, (c) 5 μm

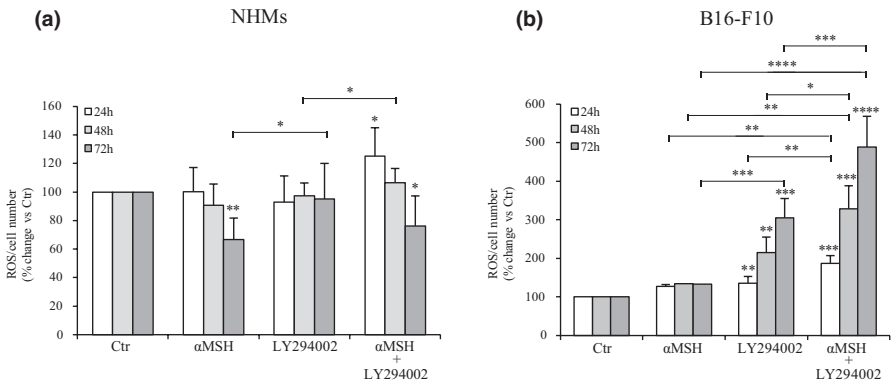

FIGURE 11 The αMSH-dependent PI3K/pAKT pathway modulates ROS production in B16-F10 and NHMs. (a,b) ROS determination in NHMs and B16-F10 treated with 10^{-7} M αMSH in the presence or absence of 10 μM LY294002 for 24, 48, and 72 hr. ROS content was normalized on cell number and expressed as percentage change versus untreated control cells. One-way ANOVA with post hoc Tukey's tests: $^{*}p < .05$, $^{**}p < .01$, $^{***}p < .001$, and $^{****}p < .0001$

apoptosis as interconnected events due to exposure to the different agents. At the 72-hr time point, LY294002 alone, in agreement with its ability to induce apoptosis (Kadekaro et al., 2005), caused significant DNA damage associated with a small, but significant, degradation of procaspase-3. This pro-apoptotic effect was even more evident at the following time points (see Figure S3). Combined treatment with αMSH plus LY294002 already induced significant DNA damage at 48 hr, and this effect was even more amplified at 72 hr. At this observation time, the degradation of procaspase-3 and therefore the commitment to apoptosis were clearly evident.

In conclusion, we showed that αMSH-dependent activation of the PI3K/AKT pathway exerts a negative feedback on melanogenesis and promotes extracellular release of melanin (see representative scheme in Figure 13). When the PI3K pathway is inhibited, melanin accumulates inside melanocytes and cells showed evidence of oxidative stress, DNA damage, and reduced survival. These findings constitute a basis for future studies, not only in the field of photo-susceptibility and predisposition to melanoma, but also for the development of innovative therapeutic approaches for melanoma.

ACKNOWLEDGMENTS

We wish to thank Marco Zaccarini of the Dermatopathological Laboratory of San Gallicano Dermatological Institute IRCCS, Rome, Italy, for the embedding and sectioning of ex vivo human skin biopsies. The present study was supported by public funds from the Italian Ministry of Health.

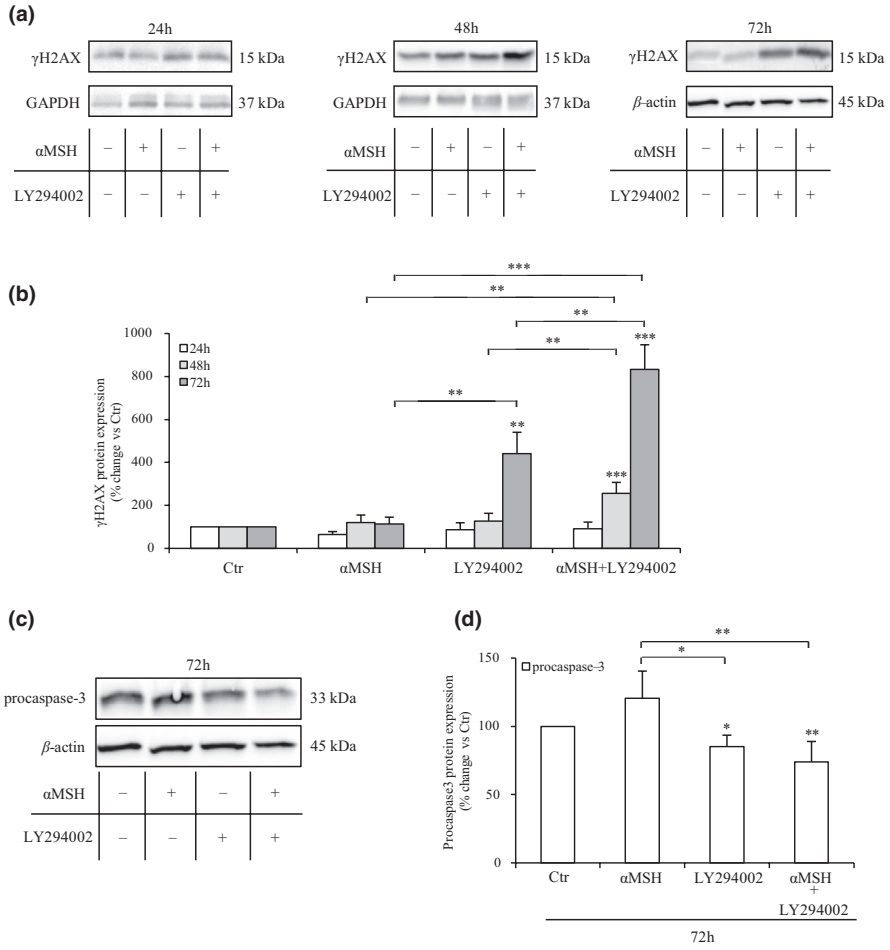

FIGURE 12 αMSH-dependent PI3K/pAKT plays a role in protecting against DNA damage and apoptosis in B16-F10. (a) Western blot analysis of γH2AX protein expression on cell lysate of B16-F10, treated with 10^{-7} M αMSH in the presence or absence of 10 μM LY294002, for 24, 48, and 72 hr. Representative blots are shown. (b) Densitometric scanning of band intensities was performed to quantify the change in protein expression. One-way ANOVA with post hoc Tukey's tests: $^{**}p < .01$ and $^{***}p < .001$. (c) Western blot analysis of procaspase-3 protein expression on cell lysate of B16-F10, treated with 10^{-7} M αMSH in the presence or absence of 10 μM LY294002, for 72 hr. Representative blot is shown. (d) Densitometric scanning of band intensities was performed to quantify the change in protein expression. One-way ANOVA with post hoc Tukey's tests: $^{**}p < .01$ and $^{**}p < .01$

CONFLICT OF INTEREST

The authors have no conflict of interest in relation to this work.

ETHICAL STATEMENT

The analyses on cultures of melanocytes of human origin were carried out on samples already present in the laboratory. The collection of new skin biopsies was approved by the Medical Ethical Committee of Institute (IFO) and was conducted according to the Principles of Declaration of Helsinki. Parents of minors and patients gave their written informed consent.

Cell cultures and treatments

The murine melanoma B16-F10 cell line, carrying a wild-type MC1R (Rusciano, Lorenzoni, & Burger, 1999), was cultured in DMEM (Euroclone, Milan, Italy) supplemented with 7% fetal bovine serum and antibiotics. Primary cultures of human melanocytes (NHMs) were set up starting from neonatal foreskin, and their expression and genetic characterization of MC1R were previously assessed and described (Flori et al., 2017). NHMs were cultured in M254-defined medium plus human melanocyte growth supplements (Invitrogen Life Technologies Italia, Monza, Italy). B16-F10 cells were plated and stimulated with chemical agents 24 hr later in fresh medium. NHMs were treated with chemicals in medium without phorbol 12-myristate 13-acetate (PMA) and bovine pituitary extract (BPE). αMSH was employed at the doses of 10^{-7} M, 10^{-8} M, or 10^{-9} M, and Wortmannin and LY294002, two PI3K inhibitors (Ohashi & Woodgett, 2005; Yu & Cui, 2016), were used at the concentration of 10 μM. In αMSH/LY294002 or αMSH/Wortmannin combined treatments, cells were pretreated with PI3K inhibitors for 1 hr. All compounds were purchased by Sigma-Aldrich S.r.l, Milan, Italy.

Ex vivo human skin model

Skin explants obtained with the informed consent of patients were cut (0.5 cm^2) and cultured on Transwell permeable supports (6.5mm diameter, 0.4 μm pore size) into standard 6-well plates at the air–liquid interface. Skin samples were cultured in defined Medium 154 (Life Technologies Italia, Monza, Italy) supplemented with Human Keratinocyte Growth Supplement (Life Technologies), 10% FBS, antibiotics, and Ca^{2+} (1.5 mM). After five days of treatments (10^{-7} M αMSH, 10 μM LY294002, and αMSH + LY294002), the explants were fixed in formalin and embedded in paraffin. Paraffin sections were stained with hematoxylin and eosin (H&E) for histomorphological analysis. For melanosome analysis, sections were incubated with anti-Melan A polyclonal antibody (Agilent Dako) overnight at + 4°C. Primary antibody was visualized with goat anti-mouse Alexa Fluor 488 conjugate antibody (1:800 in PBS) (Cell Signaling). Coverslips were mounted using ProLong Gold Antifade Reagent with DAPI (Invitrogen, Life Technologies Corporation, Oregon, USA).

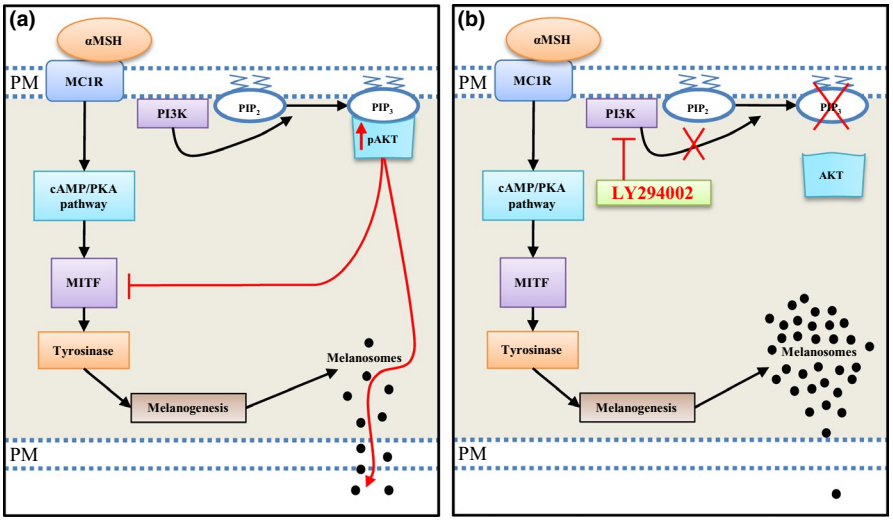

FIGURE 13 Proposed mechanism for the αMSH-dependent PI3K pathway in the control of melanogenesis and extracellular release of melanin. Red lines and red arrows indicate the events investigated in this study. (a) After stimulation with αMSH for prolonged times, we observed an increase in AKT phosphorylated levels. The increased activation of pAKT downregulates the expression of MITF and, as a consequence, leads to a decrease in the expression of tyrosinase and to a lower synthesis of melanin. Therefore, AKT phosphorylation plays a crucial role in balancing melanogenesis and the transfer of melanosomes to the extracellular space. (b) Effects due to the activation of MC1R following treatment with αMSH in the presence of LY294002, an inhibitor of PI3K. As a consequence of the combined treatment, PIP_2 is not phosphorylated to PIP_3 by PI3K, the AKT protein cannot be recruited to PM and the result is a significant decrease in the levels of AKT phosphorylation. The lack of AKT activation causes the upregulation of MITF, an increased expression of tyrosinase, and the induction of melanogenesis. The reduced levels of AKT phosphorylation also influenced the extracellular release of melanosomes, causing an intracellular accumulation of melanin clusters. αMSH, α-melanocyte-stimulating hormone; MITF, melanocyte inducing transcription factor; MC1R, melanocortin 1 receptor; PI3K, phosphoinositide 3-kinase; PIP_2, phosphatidylinositol 4,5-bisphosphate; PIP_3, phosphatidylinositol (3,4,5)-trisphosphate; PM, plasma membrane

Fluorescence signals were analyzed by recording stained images using a CCD camera (Zeiss, Oberkochen, Germany).

RNA interference experiments

For RNA interference experiments, B16-F10 cells were transfected with 100 pmols (h) Signaling Silence® AKT1 siRNA I (Mouse Specific #6909; Cell Signaling Technology, New England Biolabs, UK). An equivalent amount of non-specific siRNA (sc-44234; Santa Cruz Biotechnology, Santa Cruz, CA, USA) was used as a negative control. Cells were transfected using the Amaxa® Human Keratinocyte Nucleofector Kit (Lonza, Basel, Switzerland), according to the manufacturer's instructions. To ensure identical siRNA efficiency among the plates, cells were transfected together in a single cuvette and plated immediately after nucleofection. Twenty-four hours following transfection, treatments were added to some samples in agreement with the experimental design. Results represent the average of three independent experiments.

Tyrosinase assay

Tyrosinase activity was estimated by measuring the rate of L-DOPA (3,4-dihydroxyphenylalanine) oxidation. Briefly, cells were treated in agreement with the experimental design for 24, 48, and 72 hr. Approximately 10^7 cells were pelleted and then washed twice with phosphate-buffered saline. The supernatant was decanted after centrifugation. The cell pellet was dissolved in 1 ml of 0.5% sodium deoxycholate (Sigma) in distilled water and allowed to stand at 0°C for 15 min. Tyrosinase activity was analyzed spectrophotometrically by following the oxidation of DOPA to DOPAchrome at 475 nm. The reaction mixture, consisting of 3 ml of 0.1% L-DOPA (Sigma) in 0,1 M phosphate buffer (pH 6.8), was mixed with cell lysate (the reaction mixture was freshly prepared every 2 hr). Assays were performed at 37°C in a spectrophotometer. The rate was measured during the first 10 min of the reaction while it was linear. Corrections for auto-oxidation of L-DOPA in controls were made. Specific activity was defined as the amount of DOPAchrome formed (absorbance at 475 nm) per 10 min per cell. Two different experiments were performed.

mRNA expression analysis

RNA was extracted by the AurumTM Total RNA Mini Kit purchased from Bio-Rad Laboratories S.r.l, Milan, Italy. The amount of RNA and its degree of purity were evaluated by OD: 260/280 absorbance measurements and subsequent analysis by agarose gel electrophoresis. After digestion with DNase I, cDNA was synthesized by employing a mix of random primers and oligodT (RevertAidTM First Strand cDNA Synthesis Kit; Thermo Fisher Scientific, Monza, Italy). RT-RT-PCR was done in a volume of 10 μl with SYBR Green PCR Master Mix (Bio-Rad Laboratories S.r.l) and each primer at the concentration of 200 nM. The sequences of primers were as follows: tyrosinase sense: 5′-AGCATCCTTCTTCTCCTCCTG-3′ and antisense: 5′-GCTGAAATTGGCAGTTCTATCC-3′; GAPDH sense: 5′-TGCACCACCAACTGCTTAGC-3′; and antisense: 5′-GGCATGGACTGTGGTCATGAG-3′. Reactions were done in

triplicates by employing a CFX96 Real-time System (Bio-Rad Laboratories S.r.l). Melt curve analysis was performed to assess the specificity of products that were amplified. Relative mRNA expression was normalized to the expression of GAPDH mRNA by the change in the Δ cycle threshold (ΔCt) method and quantified on the basis of $2^{-\Delta\Delta C_t}$. Results represent the average of three independent experiments.

Immunofluorescence analysis

Cells cultured on coverslips were incubated with 10^{-7} M αMSH and 10 μM LY294002 for 24 hr. The cells were then fixed using paraformaldehyde (4% in PBS) (15 min at room temperature). The anti-pAKT rabbit antibody was used (1:100) for immunostaining. A goat anti-rabbit Alexa Fluor 555-conjugated antibody was employed (1:800) to visualize the primary antibody. All the above-described antibodies were purchased from Cell Signaling Technology, New England Biolabs, UK. ProLong Gold Antifade Reagent with DAPI was employed to mount coverslips (Invitrogen, Life Technologies Corporation, Oregon, USA). Fluorescence signals were analyzed by recording stained images using a cooled CCD color digital camera (Zeiss, Oberkochen, Germany). Quantitative analysis of fluorescence signals was performed using ZEN 2.6 software (Zeiss), evaluating at least 200 cells for each condition, randomly taken from 10 different microscopic fields in three distinct experiments. For pAKT fluorescence signals, values are expressed as fold increase in mean fluorescence intensity/cell with respect to untreated control cells (set as 100 by definition) and are reported as mean value ± *SD* (%).

Morphologic analysis by inverted phase-contrast microscope

Living cell cultures were observed daily, and images were captured by an inverted phase microscope (Olympus IX71) equipped with a digital camera in order to document cell morphologic changes after treatments. No specific staining was carried out.

Western blot analysis

The protein expression study was conducted with a conventional Western blot analysis on SDS-PAGE. The following primary antibodies were used: pAKT antibody specific for Ser473 (1:2000); AKT antibody (1:1,000); MITF antibody (1:1,000); tyrosinase antibody (1:1,000); phospho-histone H2A.X antibody (1:1,000); phospho-mTOR antibody specific for Ser2448 (1:1,000); mTOR antibody (1:1,000); pS6 antibody specific for Ser235/236 (1:2000); S6 antibody (1:1,000); procaspase-3 (1:1,000); and HRP-conjugated goat anti-rabbit IgG (1:8,000), anti-mouse (1:3,000), and anti-goat (1:1,000) were employed as secondary antibodies. All primary and secondary antibodies were purchased from Cell Signaling Technology, New England Biolabs, UK, while tyrosinase and secondary anti-goat antibody were purchased from Santa Cruz Biotechnology, CA, USA. Antibody complexes were visualized by employing the enhanced chemiluminescence reagent (ECL) (Amersham Biosciences, Milan, Italy). An hybridization with anti-β-actin antibody (1:3,000) or anti-GAPDH antibody (1:5,000) (both purchased from Santa Cruz Biotechnology Inc., Santa Cruz, CA, USA) was employed to permit equal protein loading. The densitometry of protein bands was performed by a UVITEC Imaging System (Cambridge, UK), and the modulation of protein expression was indicated as percentage change versus untreated control cells. Results represent the average of three independent experiments.

Melanin content evaluation

Cell pellets (10^6 cells) were dissolved in 0.2 M NaOH and then incubated at 65°C for 1 hr. The melanin content was evaluated at 450 nm (Barker et al., 1995) by employing a Beckman Coulter DTX 880 multimode detector (Beckman Coulter, Milan, Italy). The melanin concentration was extrapolated by interpolating raw data with a standard curve. The standard curve was generated by the absorbance of known concentrations of synthetic melanin and corrected for total protein concentration. Three determinations were done in duplicate. Obtained results were expressed as mg of melanin/ mg of proteins.

Measurement of ROS production

Cells were pretreated with drugs for 24, 48, and 72 hr. 10 μM DCFH-DA was then added to the medium. The cells were cultured in dark at 37°C for 30 min. Fluorescent intensity was immediately measured by employing a Beckman Coulter DTX 880 multimode detector (Beckman Coulter, Milan, Italy), after setting the following parameters: excitation 485 nm and emission 535 nm. ROS content was normalized on cell number. Three determinations were done in duplicate. Obtained results were expressed as % change versus untreated control cells.

Cell viability

Cells treated with different chemicals (see above) were detached by trypsinization and counted (in the presence of Trypan blue to evaluate cell viability) by a phase-contrast microscope Axiovert 40C (Zeiss, Milan, Italy). Results are the average of three experiments performed in triplicate.

Statistical analyses

Results are expressed as means ± *SD*. Comparison among groups was performed by either Student's *t* test or ANOVA followed by Tukey's multiple comparisons test using GraphPad Prism (GraphPad Software). Detail analysis of variance was reported in the legends of the figures. Statistical significance for all tests was accepted for $p < .05$.

DATA AVAILABILITY STATEMENT

The authors agree that all data reported in this study are to be made freely available to other researchers.

ORCID

Sarah Mosca http://orcid.org/0000-0002-6468-200X
Giorgia Cardinali http://orcid.org/0000-0002-7527-9451
Enrica Flori http://orcid.org/0000-0002-9275-1041
Stefania Briganti http://orcid.org/0000-0003-2000-006X
Irene Bottillo http://orcid.org/0000-0003-0396-7981

Anna M. Mileo http://orcid.org/0000-0002-1970-3297
Vittoria Maresca https://orcid.org/0000-0001-9239-6978

REFERENCES

Barker, D., Dixon, K., Medrano, E. E., Smalara, D., Im, S., Mitchell, D., … Abdel-Malek, Z. A. (1995). Comparison of the responses of human melanocytes with different melanin contents to ultraviolet B irradiation. *Cancer Research*, *55*, 4041–4046.

Brunn, G. J., Williams, J., Sabers, C., Wiederrecht, G., Lawrence, J. C. J., & Abraham, R. T. (1996). Direct inhibition of the signaling functions of the mammalian target of rapamycin by the phosphoinositide 3-kinase inhibitors, wortmannin and LY294002. *EMBO Journal*, *19*, 5256–5267. https://doi.org/10.1002/j.1460-2075.1996.tb00911.x

Burke, J. E., & Williams, R. L. (2015). Synergy in activating class I PI3Ks. *Trends in Biochemical Sciences*, *40*, 88–100. https://doi.org/10.1016/j.tibs.2014.12.003

Buscà, R., & Ballotti, R. (2000). Cyclic AMP. A key messenger in the regulation of skin pigmentation. *Pigment Cell Research*, *13*, 60–69. https://doi.org/10.1034/j.1600-0749.2000.130203.x

Buscà, R., Bertolotto, C., Ortonne, J. P., & Ballotti, R. (1996). Inhibition of the phosphatidylinositol 3-kinase/p70 (S6)-kinase pathway induces B16 melanoma cell differentiation. *Journal of Biological Chemistry*, *271*, 31824–31830.

Cao, J., Wan, L., Hacker, E., Dai, X., Lenna, S., Jimenez-Cervantes, C., … Cui, R. (2013). MC1R is a potent regulator of PTEN after UV exposure in melanocytes. *Molecular Cell*, *51*, 409–422. https://doi.org/10.1016/j.molcel.2013.08.010

Carpenter, C. L., & Cantley, L. C. (1996). Phosphoinositide 3-kinase and the regulation of cell growth. *Biochimica Biophysica Acta*, *1288*, M11–M16. https://doi.org/10.1016/0304-419X(96)00018-2

Castejón-Griñán, M., Herraiz, C., Olivares, C., Jiménez-Cervantes, C., & García-Borrón, J. C. (2018). cAMP-independent non-pigmentary actions of variant melanocortin 1 receptor: AKT-mediated activation of protective responses to oxidative DNA damage. *Oncogene*, *37*, 3631–3646. https://doi.org/10.1038/s41388-018-0216-1

Cheli, Y., Ohanna, M., Ballotti, R., & Bertolotto, C. (2010). Fifteen-year quest for microphthalmia-associated transcription factor target genes. *Pigment Cell and Melanoma Research*, *23*, 27–40. https://doi.org/10.1111/j.1755-148X.2009.00653.x

Cheng, L. B., Cheng, L., Bi, H. E., Zhang, Z. Q., Yao, J., Zhou, X. Z., & Jiang, Q. (2013). Alpha-melanocyte stimulating hormone protects retinal pigment epithelium cells from oxidative stress through activation of melanocortin 1 receptor-Akt-mTOR signaling. *Biochemical and Biophysical Research Communications*, *443*, 447–452. https://doi.org/10.1016/j.bbrc.2013.11.113

Cleary, J. M., & Shapiro, G. I. (2010). Development of phosphoinositide-3 kinase pathway inhibitors for advanced cancer. *Current Oncology Report*, *12*, 87–94. https://doi.org/10.1007/s11912-010-0091-6

Costa, C., Ebi, H., Martini, M., Beausoleil, S. A., Faber, A. C., Jakubik, C. T., … Engelman, J. A. (2015). Measurement of PIP3 levels reveals an unexpected role for p110β in early adaptive responses to p110α-specific inhibitors in luminal breast cancer. *Cancer Cell*, *27*, 97–108. https://doi.org/10.1016/j.ccell.2014.11.007

De Nicola, G. M., Karreth, F. A., Humpton, T. J., Gopinathan, A., Wei, C., Frese, K., … Tuveson, D. A. (2011). Oncogene-induced Nrf2 transcription promotes ROS detoxification and tumorigenesis. *Nature*, *475*, 106–109. https://doi.org/10.1038/nature10189

Englaro, W., Bertolotto, C., Busca, R., Brunet, A., Pages, G., Ortonne, J. P., & Ballotti, R. (1998). Inhibition of the mitogen-activated protein kinase pathway triggers B16 melanoma cell differentiation. *Journal of Biological Chemistry*, *273*, 9966–9970. https://doi.org/10.1074/jbc.273.16.9966

Flori, E., Rosati, E., Cardinali, G., Kovacs, D., Bellei, B., Picardo, M., & Maresca, V. (2017). The alpha-melanocyte stimulating hormone/peroxisome proliferator activated receptor-gamma pathway down-regulates proliferation in melanoma cell lines. *Journal of Experimental & Clinical Cancer Research*, *36*, 142. https://doi.org/10.1186/s13046-017-0611-4

Franke, T. F., Kaplan, D. R., & Cantley, L. C. (1997). PI3K: Downstream AKTion blocks apoptosis. *Cell*, *88*, 435–437. https://doi.org/10.1016/S0092-8674(00)81883-8

Herraiz, C., Garcia-Borron, J. C., Jiménez-Cervantes, C., & Olivares, C. (2017). MC1R signaling. Intracellular partners and pathophysiological implications. *Biochimica Et Biophysica Acta – Molecular Basis of Disease*, *1863*, 2448–2461. https://doi.org/10.1016/j.bbadis.2017.02.027

Herraiz, C., Journé, F., Abdel-Malek, Z., Ghanem, G., Jiménez-Cervantes, C., & García-Borrón, J. C. (2011). Signaling from the human melanocortin 1 receptor to ERK1 and ERK2 mitogen-activated protein kinases involves transactivation of cKIT. *Molecular Endocrinology*, *25*, 138–156. https://doi.org/10.1210/me.2010-0217

Kadekaro, A. L., Kavanagh, R., Kanto, H., Terzieva, S., Hauser, J., Kobayashi, N., … Abdel-Malek, Z. A. (2005). alpha-Melanocortin and endothelin-1 activate antiapoptotic pathways and reduce DNA damage in human melanocytes. *Cancer Research*, *65*, 4292–4299. https://doi.org/10.1158/0008-5472.CAN-04-4535

Khaled, M., Larribere, L., Bille, K., Ortonne, J. P., Ballotti, R., & Bertolotto, C. (2003). Microphthalmia associated transcription factor is a target of the phosphatidylinositol-3-kinase pathway. *Journal of Investigative Dermatology*, *121*, 831–836. https://doi.org/10.1046/j.1523-1747.2003.12420.x

Koundouros, N., & Poulogiannis, G. (2018). Phosphoinositide 3-Kinase/Akt signaling and redox metabolism in cancer. *Frontiers in Oncology*, *8*, 160. doi: https://doi.org/10.3389/fonc.2018.00160.

Maresca, V., Flori, E., Bellei, B., Aspite, N., Kovacs, D., & Picardo, M. (2010). MC1R stimulation by alpha-MSH induces catalase and promotes its re-distribution to the cell periphery and dendrites. *Pigment Cell & Melanoma Research*, *23*, 263–275. https://doi.org/10.1111/j.1755-148X.2010.00673.x

Maresca, V., Flori, E., Camera, E., Bellei, B., Aspite, N., Ludovici, M., … Picardo, M. (2013). Linking αMSH with PPARγ in B16–F10 melanoma. *Pigment Cell & Melanoma Research*, *26*, 113–127. https://doi.org/10.1111/j.1755-148X.2012.01042.x

Maresca, V., Flori, E., & Picardo, M. (2015). Skin phototype: A new perspective. *Pigment Cell & Melanoma Research*, *28*, 378–389. https://doi.org/10.1111/pcmr.12365

Motiani, R. K., Tanwar, J., Raja, D. A., Vashisht, A., Khanna, S., Sharma, S., … Gokhale, R. S. (2018). STIM1 activation of adenylyl cyclase 6 connects Ca^{2+} and cAMP signaling during melanogenesis. *The EMBO Journal*, *37*, e97597. https://doi.org/10.15252/embj.201797597

Ohashi, P. S., & Woodgett, J. R. (2005). Modulating autoimmunity: Pick your PI3K. *Nature Medicine*, *11*, 924–925. https://doi.org/10.1038/nm0905-924

Oka, M., Nagai, H., Ando, H., Fukunaga, M., Matsumura, M., Araki, K., … Ichihashi, M. (2000). Regulation of melanogenesis through phosphatidylinositol 3-kinase-Akt pathway in human G361 melanoma cells. *Journal of Investigative Dermatology*, *115*, 699–703. https://doi.org/10.1046/j.1523-1747.2000.00095.x

Rusciano, D., Lorenzoni, P., & Burger, M. M. (1999). Regulation of c-met expression in B16 murine melanoma cells by melanocyte stimulating hormone. *Journal of Cell Science*, *112*, 623–630.

Sánchez-Laorden, B. L., Jiménez-Cervantes, C., & García-Borrón, J. C. (2007). Regulation of human melanocortin 1 receptor signaling and trafficking by Thr-308 and Ser-316 and its alteration in variant alleles associated with red hair and skin cancer. *Journal of Biological Chemistry*, *282*, 3241–3251. https://doi.org/10.1074/jbc.M606865200

Schwartz, S., Wongvipat, J., Trigwell, C. B., Hancox, U., Carver, B. S., Rodrik-Outmezguine, V., … Rosen, N. (2015). Feedback suppression of PI3Kα signaling in PTEN-mutated tumors is relieved by selective inhibition of PI3Kβ. *Cancer Cell*, *27*, 109–122. https://doi.org/10.1016/j.ccell.2014.11.008

Sporn, M. B., & Liby, K. T. (2012). NRF2 and cancer: The good, the bad and the importance of context. *Nature Reviews. Cancer*, *12*, 564–571. https://doi.org/10.1038/nrc3278

Swope, V. B., & Abdel-Malek, Z. A. (2016). Significance of the Melanocortin 1 and Endothelin B receptors in melanocyte homeostasis and prevention of sun-induced Genotoxicity. *Frontiers in Genetics*, https://doi.org/10.3389/fgene.2016.00146

Swope, V. B., Jameson, J. A., McFarland, K. L., Supp, D. M., Miller, W. E., McGraw, D. W., … Abdel-Malek, Z. A. (2012). Defining MC1R regulation in human melanocytes by its agonist α-melanocortin and antagonists agouti signaling protein and β-defensin 3. *Journal of Investigative Dermatology*, *132*, 2255–2262. https://doi.org/10.1038/jid.2012.135

Vanhaesebroeck, B., & Alessi, D. R. (2000). The PI3K-PDK1 connection: More than just a road to PKB. *Biochemical Journal*, *346*, 561–576.

Vanhaesebroeck, B., Whitehead, M. A., & Piñero, R. (2016). Molecules in medicine mini-review: Isoforms of PI3K in biology and disease. *Journal of Molecular Medicine*, *94*, 5–11. https://doi.org/10.1007//s00109-015-1352-5

Wolf Horrell, E. M., Boulanger, M. C., & D'Orazio, J. A. (2016). Melanocortin 1 receptor: structure, function, and regulation. *Frontiers in Genetics*, *7*, 95. https://doi.org/10.3389/fgene.2016.00095

Yu, J. S., & Cui, W. (2016). Proliferation, survival and metabolism: The role of PI3K/AKT/mTOR signalling in pluripotency and cell fate determination. *Development*, *143*, 3050–3060. https://doi.org/10.1242/dev.137075

Yuan, J., Adamski, R., & Chen, J. (2010). Focus on histone variant H2AX: To be or not to be. *FEBS Letters*, *584*, 3717–3724. https://doi.org/10.1016/j.febslet.2010.05.021

SUPPORTING INFORMATION

Additional supporting information may be found online in the Supporting Information section.

How to cite this article: Mosca S, Cardinali G, Flori E, et al. The PI3K pathway induced by αMSH exerts a negative feedback on melanogenesis and contributes to the release of pigment. *Pigment Cell Melanoma Res*. 2021;34:72–88. https://doi.org/10.1111/pcmr.12910